AD_____

AWARD NUMBER: DAMD17-02-1-0652

TITLE: Role of RASGRF1 in Neurofibromatosis – Validating a Potential Therapeutic Target

PRINCIPAL INVESTIGATOR: Paul D. Soloway, Ph.D.

CONTRACTING ORGANIZATION: Cornell University
Ithaca, New York 14853

REPORT DATE: April 2006

TYPE OF REPORT: Final

PREPARED FOR: U.S. Army Medical Research and Materiel Command
Fort Detrick, Maryland 21702-5012

REPORT DOCUMENTATION PAGE

Form Approved
OMB No. 0704-0188

1. REPORT DATE *(DD-MM-YYYY)*	**2. REPORT TYPE**	**3. DATES COVERED** *(From - To)*
01-04-2006	Final	1 Jun 2002 – 31 Mar 2006

4. TITLE AND SUBTITLE

Role of RASGRF1 in Neurofibromatosis – Validating a Potential Therapeutic Target

5a. CONTRACT NUMBER

5b. GRANT NUMBER
DAMD17-02-1-0652

5c. PROGRAM ELEMENT NUMBER

6. AUTHOR(S)

Paul D. Soloway, Ph.D.

E-Mail: pds28@cornell.edu

5d. PROJECT NUMBER

5e. TASK NUMBER

5f. WORK UNIT NUMBER

7. PERFORMING ORGANIZATION NAME(S) AND ADDRESS(ES)

Cornell University
Ithaca, New York 14853

8. PERFORMING ORGANIZATION REPORT NUMBER

9. SPONSORING / MONITORING AGENCY NAME(S) AND ADDRESS(ES)
U.S. Army Medical Research and Materiel Command
Fort Detrick, Maryland 21702-5012

10. SPONSOR/MONITOR'S ACRONYM(S)

11. SPONSOR/MONITOR'S REPORT NUMBER(S)

12. DISTRIBUTION / AVAILABILITY STATEMENT
Approved for Public Release; Distribution Unlimited

13. SUPPLEMENTARY NOTES

14. ABSTRACT

It was hypothesized that the gene encoding the RASGRF1 protein, a GTP exchange factor (GEF), controls the severity of neurofibromatosis. Over-expression of the Rasgrf1 gene was predicted to exacerbate neurofibromatosis while Rasgrf1 silencing will attenuate it. Two novel strains of mice ideally suited to test this hypothesis that were developed in my lab were used to evaluate the role or RASGRF1 on the manisfestations of neurofibromatosis type 1. One strain of mice over-express Rasgrf1, the other has diminished expression. These were crossed with a mouse model for NF1 and the effects of the altered level of RASGRF1 protein on tumorigenesis were monitored. The results of these studies support the hypothesis that attenuating the GEF activity of RASGRF1 protein also attenuates tumorigenic pathways controlled by NF1. Also, in characterizing the strains of mice we developed for this study, we obtained new insights into the regulation and functions of the Rasgrf1 gene.

15. SUBJECT TERMS
RASGRF1, exchange factor, RAS activation, p53, NF1, mouse model

16. SECURITY CLASSIFICATION OF:			**17. LIMITATION OF ABSTRACT**	**18. NUMBER OF PAGES**	**19a. NAME OF RESPONSIBLE PERSON**
a. REPORT	**b. ABSTRACT**	**c. THIS PAGE**			USAMRMC
U	U	U	UU	15	**19b. TELEPHONE NUMBER** *(include area code)*

Table of Contents

INTRODUCTION:

It was hypothesized that the gene encoding the RASGRF1 protein, a GTP exchange factor (GEF), controls the severity of neurofibromatosis. Over-expression of the *Rasgrf1* gene was predicted to exacerbate neurofibromatosis while *Rasgrf1* silencing will attenuate it. Two novel strains of mice ideally suited to test this hypothesis that were developed in my lab were used to evaluate the role or RASGRF1 on the manisfestations of neurofibromatosis type 1. One strain of mice over-express *Rasgrf1*, the other has diminished expression. These were crossed with a mouse model for NF1 and the effects of the altered level of RASGRF1 protein on tumorigenesis were monitored. The results of these studies support the hypothesis that attenuating the GEF activity of RASGRF1 protein also attenuates tumorigenic pathways controlled by NF1. Also, in characterizing the strains of mice we developed for this study, we obtained new insights into the regulation and functions of the *Rasgrf1* gene. This final report is a comprehensive description of the results of this project. These results are reported for each of the tasks or Aims originally approved. Where additional data related to the approved aims were obtained, these are included as well.

BODY:

AIM 1: Do *Rasgrf1* expression levels affect tumorigenesis in a mouse model for neurofibromatosis? In this central Aim, it will be determined if *Rasgrf1* expression levels affect the manifestations of neurofibromatosis. Mice with ablated or enhanced expression of *Rasgrf1* will be crossed with mice harboring mutations in *Nf1* and *p53* which predisposes them to tumors associated with neurofibromatosis. The progeny of these crosses will be evaluated for tumor development and progression. If RASGRF1 levels affect tumor development, it will be revealed in this analysis. Suppression of tumorigenesis in mice lacking RASGRF1would validate RASGRF1 as target for therapeutic intervention in neurofibromatosis.

An important control for our work was to document directly the altered levels of *Rasgrf1* expression in our mutant mice used in this study. To do this, we performed real time PCR assays. RNA was isolated from whole brains of mutant mice at different developmental stages, cDNAs prepared and real time PCR performed using TaqMan probes for fluorescence detection. The graphs in figure 1 show the results with the Y axis reporting the C_T values of the real time PCR which reflect the relative abundance of *Rasgrf1* RNAs from the mice. Note that high C_T values reflected low mRNA abundance and for every unit difference in C_T value, there is a two fold difference in mRNA abundance. BJR2/+ mice are the animals with biallelic expression of *Rasgrf1*, +/+ are wild type mice with paternal allele-specific expression and +/BJR3 mice lack expression from the single normally active paternal allele in neonates. The data show that levels of *Rasgrf1* RNA are only slightly higher in BJR2/+ than in +/+ neonates, despite the biallelic expression in the former while level in +/BJR3, the *Rasgrf1* RNA level is approximately 5% of that seen in the other two strains of mice. In adult brain, BJR2/+ mice had the highest level of *Rasgrf1*expression which was twice that seen in +/+ animals which was in turn twice that seen in +/BJR3 mice.

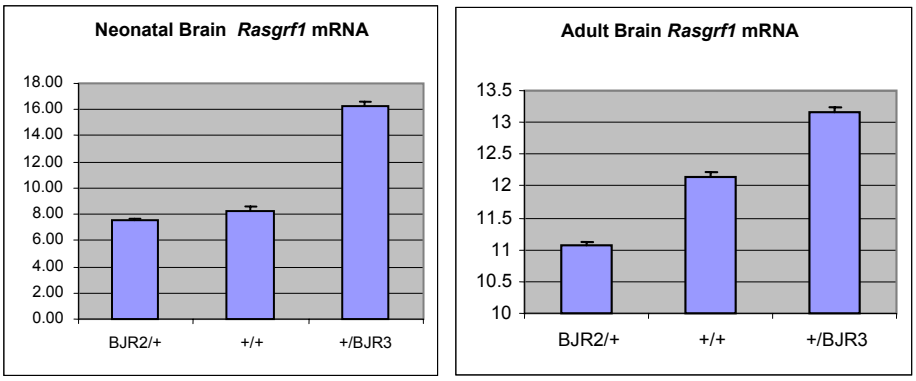

Figure 1. Real time PCR results for assays of *Rasgrf1* mRNA from mice. The y-axis shows Ct values. Low Ct values indicate high levels of expression while high Ct values indicate low levels of expression. Each Ct unit indicates a two-fold difference in expression.

To test the influence or RASGRF1 on the manisfestations of neurofibromatosis type 1, we established crosses between a mouse model for NF1 and our mice that over- or under-express *Rasgrf1* (*1, 2*). The NF1 model used is the so called “NP-cis” mice with lesions at *Nf1* and *p53* seven centimorgans apart on the same chromosome (*3*) Genotypic analysis of the progeny from this cross was done for *Nf1*, *p53* and the two separate alleles of *Rasgrf1*. A total of 123 animals were generated that included 75 with the original NP-cis genotype (NP), 25 mice with the NP-cis allele that also

over-express *Rasgrf1* due to an activating mutation on the normally silent maternal allele (NP2) and 23 with the NP-cis allele that also under-express *Rasgrf1* due to an inactivating mutation on the single active paternal allele (NP3) and. The crosses were done in a manner that produced strain matched individuals so that the analysis of tumor incidence would not be confounded by strain background effects. All animals were monitored for 10 months after birth for signs of tumor formation. Mice were sacrificed shortly after tumor onset. The results indicate that over-expression of *Rasgrf1* in the NP2 animals significantly hastens the time of tumor onset and increases the overall frequency of tumor incidence. In contrast, diminished expression modestly delays the timing of tumor development, but overall frequency of tumor development is not changed (figure 2). These results demonstrate that *Rasgrf1* over-expression is a risk factor for tumorigenesis associated with the NP-cis mouse model of neurofibromatosis type 1.

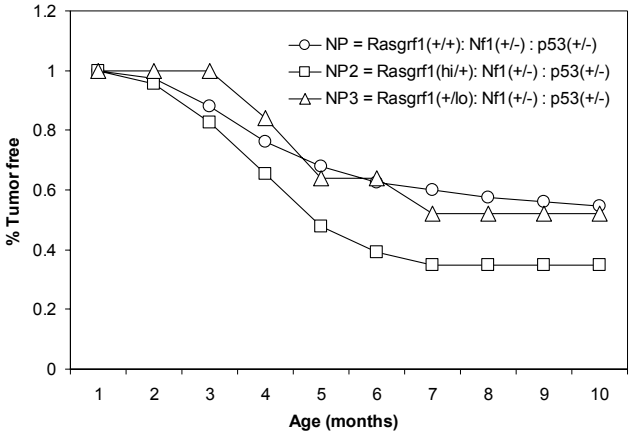

Figure 2. NP-cis mice (NP (*3*)) on the 129Sv background were bred with *Rasgrf1* mutant animals, also on the 129Sv background. Crosses involved mice with the BJR2/+ mutation described in figure 1 that have high levels of *Rasgrf1* expression (*2*). BJR2/+ mutants are referred to in this figure as Rasgrf1 (hi/+) to indicate their high levels of *Rasgrf1* expression. Progeny of this cross that harbor both the *p33* and *Nf1* mutations in *cis*, and the *Rasgrf1* (hi/+) mutation are called NP2. Parallel crosses were done between mice with the +/BJR3 mutation described in figure 1 that have low levels of *Rasgrf1* expression (*1*). +/BJR3 mutants are referred to in this figure as Rasgrf1 (+/lo) to indicate low levels of *Rasgrf1* expression. Progeny of this cross that harbor both the *p33* and *Nf1* mutations in *cis*, and the *Rasgrf1* (+/lo) mutation are called NP3.

One of the consequences of neurofibromatosis is altered mental capacity in affected individuals. Though not originally proposed, we chose to explore more thoroughly another key feature of neurofibromatosis that may be affected by altered *Rasgrf1* expression – namely learning and behavioral manifestations. These extend beyond issues limited to tumorigenesis and relate to quality of life issues for patients. One behavioral test that was established was designed to evaluate learning and memory in neonates with perturbed *Rasgrf1* expression. We performed a set of studies using our mouse models to evaluate how changes in *Rasgrf1*expression altered cognitive functions. The paradigm involved training neonatal pups with altered *Rasgrf1* expression to recognize an odorant associated with their mother, then testing their tendency to move towards the mother-associated odor when they were hungry and wished to nurse. Five day old mice were separated from their mothers for one hour, during which time the mothers were scented with an odorant (rewarded odor). Upon return of pups to their mothers, they nursed and could detect the rewarded odor. At 8 days of age, mice were separated from the mothers for another hour then tested in a chamber that presented the rewarded odor and a related but distinct neutral odor. The time, in seconds, spent in each sector of the chamber where the odors were concentrated was measured. The results show that deficiency in *Rasgrf1*expression impaired the ability of pups to recognize odors associated with their mothers, while animals over expressing *Rasgrf1* had a normal capacity to identify maternal odors (figure 3). Controls were done to ensure there were no inherent locomotion defects or odor preferences for the genotypes. These data do not distinguish between failure of low *Rasgrf1* expressing mice to learn the maternal scent and lower motivation of mice to locate the maternal scent. While high *Rasgrf1* expression exacerbates one manifestation of neurofibromatosis as hypothesized – namely severity of the tumor phenotype, it does not apparently affect another manifestation – namely impaired cognitive function. Instead it appears that loss of *Rasgrf1* that impairs cognition. This is consistent with the reports of others (*4*).

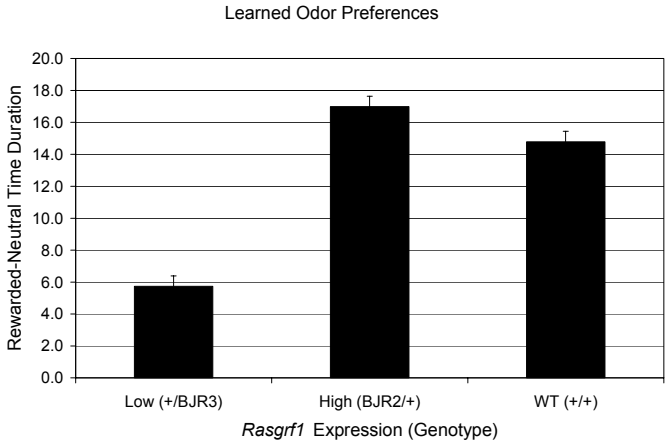

Figure 3. Time in seconds spent in the rewarded scent zone minus time spent in the unrewarded scent zone for mice with low, high or normal, wild type (WT) levels of *Rasgrf1* expression. Values reported are ± standard error. Lower than wild type values indicate an impaired ability to learn maternal scent or impaired motivation to locate the maternal scent.

AIM 2: Is the activation status of Ras affected by altered *Rasgrf1* expression and do any changes affect downstream signaling in the MAP kinase pathway? *In vitro* studies have shown that *Rasgrf1* stimulates Ras activation and MAP kinase pathway signaling. In this Aim, Ras activation and MAP kinase signaling will be analyzed in mutant mice produced in Aim 1. This will elucidate the molecular consequences of altered *Rasgrf1* expression *in vivo* which will be correlated with the tumor outcomes in the various mutants.

Because there are differences in the amount of expression in the brains of mice of the GTP exchange factor *Rasgrf1*, we wished to measure the extent of Ras activation as measured by the GTP-bound form of Ras. This was measured by a pull down assay using Raf-bound agarose beads – Raf preferentially binds Ras when it is in its GTP-bound state. The pulled down material was detected by Western blot and as a control for loading, the total amount of Ras in the input sample before pull down was measured as well. The results shown in figure 4 reveal no differences in Ras activation status or total Ras levels among +/+, BJR2/+ or +/BJR3 mice. It is not clear what other signaling pathways may be modified by altered *Rasgrf1* expression, however, they clearly do not seem to involve total Ras. This suggests that the effects of RASGRF1 protein on the manifestations of neurofibromatosis shown in figure 2 do not involve an influence of RASGRF1 GEF activity on the net activation state of total cellular Ras. It is possible that specific isoforms of Ras, namely N-Ras or R-Ras are selectively affected and these are not detected when total Ras activation is queried as done in this experiment. Alternatively, a separate signaling pathway like Rac may be affected.

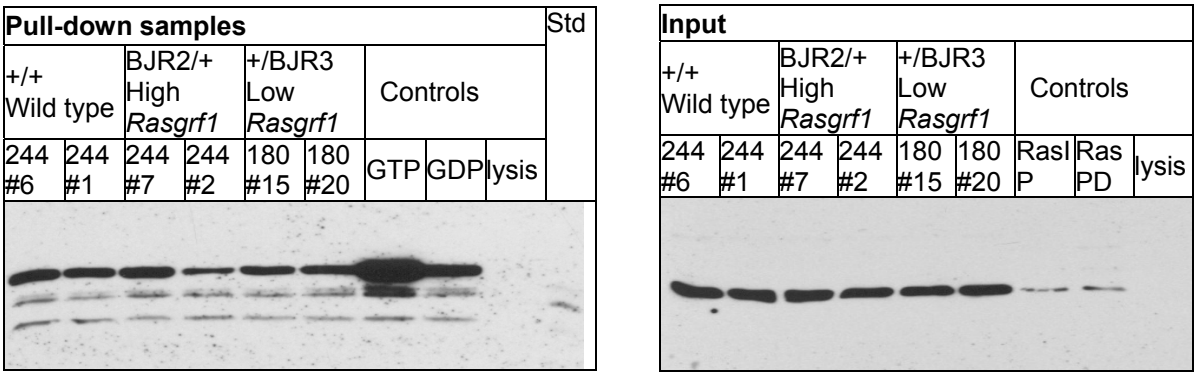

Figure 4. Ras activation status in +/+ (normal expression), BJR2/+ (slight over expression) and +/BJR3 (no expression) mice. Whole brain lysates from duplicate brains of mice were subjected to Raf-mediated pull down of Ras-GTP followed by Western blot analysis of Ras protein (left). The identifying numbers of each mouse are indicated. Controls included lysis buffer alone, or +/+ extracts incubated with GTP or GDP which demonstrated GTP incubation could enhance the activation status of Ras. Total lysates of each sample prior to pull down were also assayed by Western blot (right) for each mouse tested which revealed no significant differences among the mice. Controls included Ras protein that had been isolated by immune precipitation (IP) and also by Raf pull down (PD). Lysis buffer alone was included as a negative control.

AIM 3: What are the *Rasgrf1* expression patterns in normal and cancerous tissues from the peripheral nervous system (PNS) and tissues supporting the PNS?

Rasgrf1 is expressed virtually ubiquitously, with highest levels of expression in neurons of the central nervous system. However, expression patterns in the PNS or in tissues supporting the PNS have not been thoroughly examined. These tissues are sites of formation of tumors associated with neurofibromatosis. To evaluate levels of RASGRF1 protein in normal and cancerous tissue we performed immunohistochemistry (IHC) using commercially available antibody (sc-224 from Santa Cruz Biotech). Initial tests were done using brain tissue from our wild type, BJR2/+ high *Rasgrf1* and +/BJR3 low expressing mice. Sections were also counterstained with either propidium iodide to detect nuclei, MAP2 antibody to detect astrocytes or NSE to detect neurons. As an additional and critical set of controls for antibody specificity, we used tissue from high expressing mice as a positive control and from low expressing mice as a negative control. We also blocked the antibody reaction using the RASGRF1 peptide against which the polycolonal antibody was prepared. Our results with these controls showed an unacceptable level of background staining from our antibody (figure 5). While ICH was considered a better means of detecting RASGRF1 protein, the antibody reagent was unreliable.

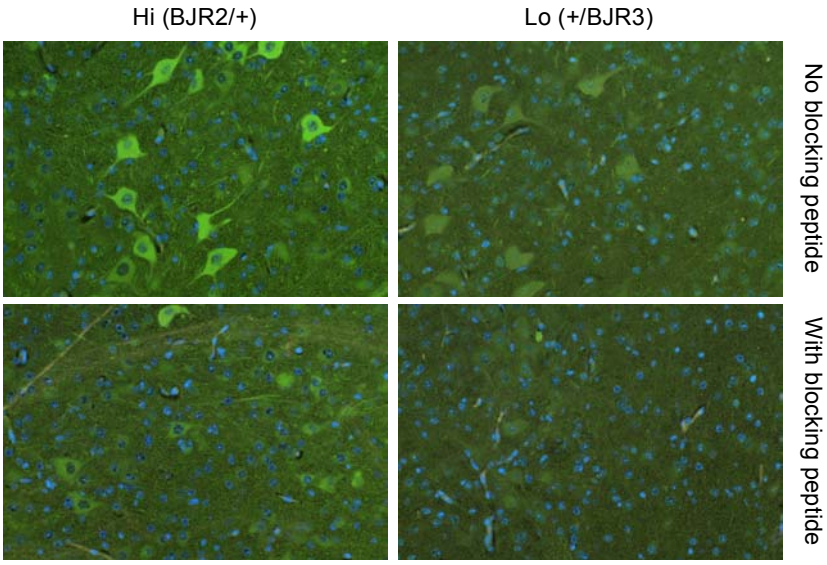

Figure 5. Immunohistochemistry of RASGRF1. Brains of neonatal mice with high [Hi (BJR2/+)] or low [Lo (+/BJR3)] levels of *Rasgrf1* mRNA were fixed in 4% paraformadehyde, embedded in paraffin and sectioned. Sections fixed on slides were de-paraffinized, antigens retrieved by microwaving in phosphate buffer and stained with rabbit anti RASGRF1 as the primary antibody (sc-224 from Santa Cruz Biotech). Counterstaining was done with secondary FITC-labeled antirabbit sera and DAPI to counterstain nuclei. The primary antibody was incubated with sections in the absence (No blocking peptide) or presence (With blocking peptide) using the peptide against which the polyclonal serum was raised. The residual green staining in the lower left panel and upper right panel reflect non-specific staining unrelated to RASGRF1.

We considered the possibility that the cross reacting antigen was RASGRF2. To test this, we performed the immunoprecipitation (IP) and Western blot shown in figure 6, using the sc-224 antibody from Santa Cruz Biotech in both the IP and the Western. The blot revealed a species migrating where RASGRF2 was expected. This verified cross reaction is the likely basis of the IHC failure. However the analysis did reveal that there are at least 2 RASGRF1-interacting proteins that could be detected by IP that may be relevant to RASGRF1 function.

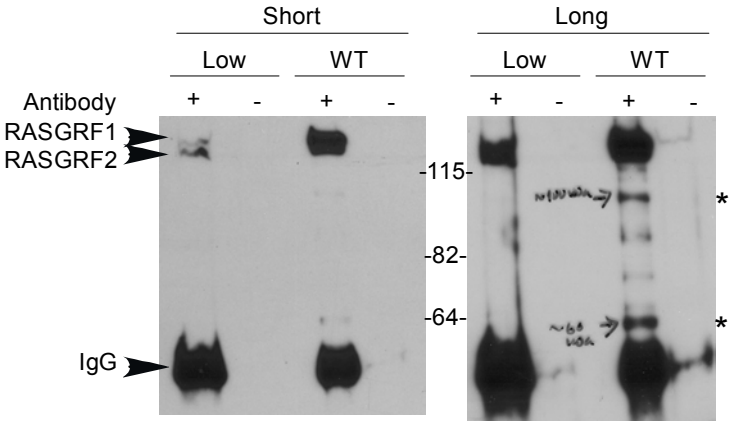

Figure 6. Immunoprecipitation followed by Western blot of brain extracts from mice expressing low levels of RASGRF1 (Low, +/BJR3) and wild type levels (WT, +/+). Immunoprecipitation reactionss were done with anti RASGRF1 antibody (+) from Santa Cruz Biotech (sc-244) or without antibody (-). The same anti RASGRF1 antibody was use for Western analysis. RASGRF1 and RASGRF2 do not resolve in WT immunoprecipitates but the low abundance of RASGRF1 in the Low expressers reveals the separate and faster migrating RASGRF2 band. IgG that is non-specifically detected in the Western blot and molecular weight markers in kiloDaltons are shown. The two asterisks indicate position of putative RASGRF1 interacting proteins. Note that they are detected only in the WT extracts and not in the Low RASGRF1 extracts. Short and Long indicate Western blot exposure times.

KEY RESEARCH ACCOMPLISHMENTS:

- Validated the hypothesis that RASGRF1 participates in the tumorigenic manifestations of neurofibromatosis as its over expression exacerbates tumor phenotypes caused by NF1 loss. However, because *Rasgrf1* under expression does not alleviate the tumor outcome, it is unlikely to be a useful therapeutic target for treating tumor manifestations of neurofibromatosis. So while RASGRF1 can participate in neurofibromatosis when its expression is up-regulated, RASGRF1 loss does not limit the rate of tumor formation or progression.
- Demonstrated that an increase in total Ras activation state is not the basis of increased tumor incidence in mice with elevated *Rasgrf1* expression. This indicates that alternate signaling pathways are targets for RASGRF1.
- Demonstrated that loss of *Rasgrf1* leads to behavioral phenotypes, impairing normal behaviors. This indicates possible undesirable behavioral side-effects may accompany any therapeutic strategies to treat neurofibromatosis with RASGRF1 antagonists.
- Identified putative RASGRF1-interacting proteins.

REPORTABLE OUTCOMES:

- Lee, M. and Soloway, P.D., *Attenuation of neurofibromatosis-related tumor phenotypes caused by loss of Rasgrf1,* Manuscript in Preparation
- Cleland, T., Drake, H., DeVito, L. and Soloway, P.D. *Impaired maternal preference/recognition caused by loss of Rasgrf1* Manuscript in Preparation.
- Published manuscript found in appendix B.-J. Yoon *et al.*, *Mol Cell Biol* **25**, 11184–11190 (2005).
- Ph.D. earned by Dr. Marie Lee was supported in part by this funding.

CONCLUSION:

The key outcome of this study is that amplification of RASGRF1 activity in mice can amplify the frequency of tumor development in a model of neurofibromatosis, however, loss of RASGRF1 activity will not serve to limit neurofibroma development in this model. Furthermore, any efforts to attenuate RASGRF1 activity for therapeutic benefit may be accompanied by unintended behavioral consequences, impairing normal behaviors.

REFERENCES:

1. B. J. Yoon *et al.*, *Nat Genet* **30**, 92-6 (Jan, 2002).
2. B.-J. Yoon *et al.*, *Mol Cell Biol* **25**, 11184–11190 (2005).
3. K. S. Vogel *et al.*, *Science* **286**, 2176-9 (1999).
4. R. Brambilla *et al.*, *Nature* **390**, 281-6 (1997).

APPENDICES:

Reprint of B.-J. Yoon *et al.*, *Mol Cell Biol* **25**, 11184–11190 (2005).

MOLECULAR AND CELLULAR BIOLOGY, Dec. 2005, p. 11184–11190 Vol. 25, No. 24
0270-7306/05/$08.00+0 doi:10.1128/MCB.25.24.11184–11190.2005

Rasgrf1 Imprinting Is Regulated by a CTCF-Dependent Methylation-Sensitive Enhancer Blocker

Bongjune Yoon,[1]†‡ Herry Herman,[1,2,3]† Benjamin Hu,[2] Yoon Jung Park,[2] Anders Lindroth,[2] Adam Bell,[4]§ Adam G. West,[4]¶ Yanjie Chang,[1] Aimee Stablewski,[1] Jessica C. Piel,[2]‖ Dmitri I. Loukinov,[5] Victor V. Lobanenkov,[5] and Paul D. Soloway[1,2]*

Department of Molecular and Cellular Biology, Roswell Park Cancer Institute, Buffalo, New York 14263[1]; Division of Nutritional Sciences, 108 Savage Hall, Cornell University, Ithaca, New York 14853[2]; Department of Orthopaedic Surgery, School of Medicine, Padjadjaran State University-Hasan Sadikin General Hospital, Bandung, West Java, Indonesia[3]; Laboratory of Molecular Biology, NIDDK, NIH, Bethesda, Maryland 20892[4]; and Laboratory of Immunopathology, NIAID, Rockville, Maryland 20852[5]

Received 2 May 2005/Returned for modification 13 June 2005/Accepted 3 October 2005

Imprinted methylation of the paternal *Rasgrf1* allele in mice occurs at a differentially methylated domain (DMD) 30 kbp 5′ of the promoter. A repeated sequence 3′ of the DMD regulates imprinted methylation, which is required for imprinted expression. Here we identify the mechanism by which methylation controls imprinting. The DMD is an enhancer blocker that binds CTCF in a methylation-sensitive manner. CTCF bound to the unmethylated maternal allele silences expression. CTCF binding to the paternal allele is prevented by repeat-mediated methylation, allowing expression. Optimal in vitro enhancer-blocking activity requires CTCF binding sites. The enhancer blocker can be bypassed in vivo and imprinting abolished by placing an extra enhancer proximal to the promoter. Together, the repeats and the DMD constitute a binary switch that regulates *Rasgrf1* imprinting.

Approximately 70 transcripts undergo genomic imprinting, in which expression is primarily or exclusively from one parental allele while the other allele remains silent. Accompanying allele-specific expression is allele-specific DNA methylation, which is important for imprinted expression (17). In mice, the paternal *Rasgrf1* allele is exclusively expressed in neonatal brain, while the maternal allele is silent. The paternal allele is also methylated within a differentially methylated domain (DMD) located 30 kbp 5′ of the promoter. Immediately 3′ of the DMD is a repeated sequence element containing 40 copies of a 41-nucleotide (nt) element. DMD methylation requires the repeats. Mice lacking the repeats on the paternal allele fail to establish proper paternal specific DNA methylation during gametogenesis (11, 29). Removal of the paternal repeats after fertilization but before implantation causes a loss of previously established methylation (R. Holmes, Y. Chang, and P. D. Soloway, submitted for publication). Collectively, the results show the *Rasgrf1* repeats provide a positive signal for establishing and maintaining DNA methylation in mice. In other studies, sequences have been identified that regulate methylation at transgene insertion sites (4, 5, 15) and at the endogenous position of the imprinted *H19*/*Igf2* locus (8, 25, 27).

Paternal allele-specific expression of *Rasgrf1* in neonatal brain requires DMD methylation. Mutations that cause inappropriate loss of paternal allele methylation silence paternal allele expression, while mutations that induce maternal allele methylation activate the normally silent maternal allele (11, 29; Holmes et al., submitted). The correlation between DMD methylation and expression at *Rasgrf1* is reminiscent of the relationship between methylation of the *H19* DMD and expression of the tightly linked *Igf2* locus. The *H19* DMD is a methylation-sensitive enhancer-blocking element that binds CTCF when unmethylated, as on the maternal allele. This enables the enhancer-blocking activity of the DMD to prevent interaction between a downstream enhancer with the upstream *Igf2* promoter, thus silencing the maternal *Igf2* allele. However, when the DMD is methylated, as on the paternal allele, two things occur: methylation spreads to the *H19* promoter, preventing *H19* transcription, and CTCF can no longer bind the DMD. Because CTCF binding is required for enhancer-blocking activity, its absence from the methylated paternal allele permits interaction between the downstream enhancer and the upstream *Igf2* promoter, allowing expression of the paternal allele (2, 10, 13). We show that a similar mechanism applies to regulation of *Rasgrf1* imprinting. These data, combined with our identification of *cis*-acting sequences controlling DNA methylation, provide a detailed model describing regulation of imprinting at *Rasgrf1*.

MATERIALS AND METHODS

Enhancer blocking assays. We performed enhancer blocking assays as described previously, inserting all test fragments into the AscI or SalI sites of pNI or slightly altered derivatives (3). The DMD repeat sequence was on a 2,103-bp

* Corresponding author. Mailing address: Cornell University, Div. of Nutritional Sciences, 108 Savage Hall, Ithaca, NY 14853. Phone and fax: (607) 254-6444. E-mail: pds28@cornell.edu.

† These authors contributed equally and are listed chronologically with respect to their contributions.

‡ Present address: MIT Picower Center, Cambridge, MA 02139.

§ Present address: Human Genome Sciences, Inc., Rockville, MD 20850.

¶ Present address: Division of Cancer Sciences and Molecular Pathology, University of Glasgow, Western Infirmary, Glasgow G11 6NT, United Kingdom.

‖ Present address: University of California at Berkeley, Berkeley, CA 94720.

EcoRI-to-EcoRV fragment. The DMD was amplified using primers, DMD FORWD (5′-TTGGCGCGCCGGACTCTTCAGAGAGTATGTAAAGCC-3′) and 92BRASC (5′-TTGGCGCGCCGAAGTGCGGCAGCAGCAGCGATA GC-3′), to generate a 349-bp product. This PCR product was cloned, sequence was verified, and mutations were prepared at positions 160, 230, and 320, where a 5′-GCnGCCnC-3′ consensus sequence shared with CTCF sites from *H19* was found using a QuickChange kit (Stratagene). The position 160 consensus was changed from 5′-GCGGCCGC-3′ to 5′-ATGATTGT-3′ using oligonucleotides 5′-TCATGATTGTGCTGCTGCTCCCACATCC-3′ and 5′-GCACAATCA TGAAACGGTAGCGAAGTGC-3′; the position 230 consensus was changed from 5′-GCTGCCGC-3′ to 5′-ATTATTGT-3′ using oligonucleotides 5′-CCA TTATTGTTAAGCTATGGCTGCCGCA-3′ and 5′-TAACAATAATGGTGC AGCAACAGCAATA-3′; the position 320 consensus was changed from 5′-GCT GCCGC-3′ to 5′-ATTATTGT-3′ using oligonucleotides 5′ CGATTATTGTGC TATCGCTGCTGCTGCC-3′ and 5′-GCACAATAATCGTAGCGCAACGGT AGTG-3′.

Gel shift analysis. We performed the gel shift analysis shown in Fig. 2A and B as described previously (3). Binding reactions included 5 μg of partially purified chicken CTCF or chicken erythrocyte extracts, 20 mM HEPES, pH 7.9, 150 mM KCl, 5 mM $MgCl_2$, 5% glycerol, 1 mM dithiothreitol, 0.5% triton X-100, 50 ng/μl poly(dA-dT), and 20 fmol labeled oligonucleotide probe. Oligonucleotide probes include some described earlier (2, 3) or double-stranded forms of the following primers labeled with polynucleotide kinase prior to annealing to the complement: DMD160 (5′-AGGCGCGCCCTGCTGCCGCGCTTCGCGCCT GCACTTCGCTACCGTTTCGCGGCCGCGCTGCTGCTC CCACATCCATCCGGGCGCGCCT-3′), DMD230 (5′-AGGCGCGCCTCC ATCCGTGGCTACCGCTATTGCTGTTGCTGCACCGCTGCCGCTAAG CTATGGCTGCCGCACTTCACTGGGCGCGCCT-3′), and DMD320 (5′-AGG CGCGCCCCACGACTGCTACTGCTGCTGCTGCACTACCGTTGCGCT ACGGCTGCCGCGCTATCGCTGCTGCTGCCGCGGCGCGCCT-3′). 320m was DMD320 synthesized with methylcytosines at the eight CG dinucleotides. Incubation was at room temperature for 45 min, and products were run on a 5% (29:1, acrylamide-bisacrylamide) gel in 1× Tris-borate-EDTA at 150 V for 1.5 to 2 h.

The gel shift analysis shown in Fig. 2C, D, and E, using PCR-generated probes, was done as described previously (9). Briefly, binding reactions were at room temperature in a 20-μl volume and included 5 μg in vitro-transcribed and -translated full-length CTCF, the CTCF Zn finger fragment, or luciferase as a negative control and labeled probe in 5 mM $MgCl_2$, 0.65 mM $ZnSO_4$, 0.35 mM β-mercaptoethanol, 7.5% glycerol, 0.065% NP-40, 2.5 μg/ml salmon sperm DNA, and 50 μg/ml poly(dI-dC). We used the following primers to PCR amplify probes used in Fig. 2C, D, and E using cloned fragments as templates: 160 was amplified with P2F (5′-GGAATTCTGGGGACTCTTCAGAGAGTTT-3′) and P2R (5′-CGGTAGCCACGGATGGATGTGGG-3′); 230 was amplified with P3F (5′-CTTCGCTACCGTTTCGCGGCC-3′) and P3R (5′-GGTAGTTGT AGCGCAGCGGTAGCG-3′); 320 was amplified with P4F (5′-GCTGCACCG CTGCCGCTAAG-3′) and P4R (5′-CAGCACGGCAGCGAAGTGCGG-3′). We methylated PCR products with SssI methyltransferase and verified the extent of methylation by digestion overnight with BstUI restriction endonuclease. The *XIST* probe was described previously (24). Reactions were electrophoresed on 5% polyacrylamide gels run in 0.5× Tris-borate-EDTA buffer.

ChIP. For chromatin immunoprecipitation (ChIP) analysis, we used established protocols (http://www.upstate.com/misc/protocols.q.prot.e.chips/Chromatin+Immunoprecipitation++ChIPs++Assay+Kit) with modifications. Briefly, we fixed approximately 1×10^7 cells by adding formaldehyde (1% volume basis) to the medium for 10 min at room temperature with agitation followed by a 10-min quench with 0.5 M glycine. After washing cells twice with 50 ml phosphate-buffered saline (PBS) containing Roche Complete proteinase inhibitor (catalog no. 11697498001), reconstituted as recommended by the manufacturer, we collected cells in 2 ml ice-cold PBS with proteinase inhibitor, centrifuged cells, and resuspended them in the same solution at a concentration of 1×10^7 cells per ml. We sonicated cells to shear the DNA into 700-bp fragments, diluted with 9 volumes of PBS with proteinase inhibitor, and then performed the immunoprecipitation on one-quarter of the lysate using anti-CTCF antibody (Abcam catalog no. 06-917). As a negative control, antibody was omitted. After the final washes of the precipitate, elution of the CTCF-DNA complex, and reversal of the cross-links, we performed real-time PCR to detect the amount of bound wild-type DNA using primers P2F and P6R described above.

Methylation analysis of cells used in ChIP studies. DNA templates were amplified using primers PDS12 (5′-CACATCCATCCGTGGCTACCGCTA TTGCTGT-3′) and PDS13 (5′-GCGAAGTGCGGCAGCAGCAGCGA-3′), which span five HhaI sites in the DMD. Real-time PCRs including SYBR green were done with an ABI 7500 instrument.

Development and characterization of mutant mice. We prepared the *Rasgrf1*^{tm2Pds} targeting vector, pBJR2, as follows. We amplified, by PCR, a 2-kbp 5′ homologous arm using a 7-kbp BamHI genomic clone with sequences 5′ of the repeats as a template. The forward primer (5′-CATGCTCCTTGGGATGTT GA-3′) was from the plasmid pSPL3, in which the BamHI fragment was cloned; the reverse primer (5′-CGAAGTGCGGC**T**GCAG**A**AGC**TT**TAGCGCGGCAG CCGTAGCG-3′) was located at the 5′ junction of the repeat. The reverse primer differed from the wild type at three nucleotide positions to generate PstI and HindIII sites specific for the mutated allele (mutated sequences are in bold). We placed 3′ of this a 1.5-kbp *neo* cassette and a 500-nt *Pgk* enhancer-and-promoter fragment in reverse orientation that replaced the *Rasgrf1* repeats. The 3′ homologous arm was a 3-kbp EcoRV-to-BamHI fragment located 3′ of the repeats. The BRP1.0 probe used for Southern blots was located 5′ of the 5′ arm. We used standard methods for embryonic stem cell culture and blastocyst injections. Southern blots for methylation analysis and reverse transcriptase PCR for expression analysis were described previously (29). All animal research complied with all relevant federal guidelines and institutional policies.

RESULTS

Enhancer blocking elements at *Rasgrf1*. We tested the *Rasgrf1* DMD and repeat-containing sequences for enhancer-blocking activity using a previously described assay (3, 6). The system utilized the chicken β-globin enhancer augmenting transcription of a *neo* reporter by a weak human ^{A}γ-globin promoter. We placed sequences to be tested in either orientation between the enhancer and promoter or outside the enhancer-to-promoter interval, electroporated these into K562 human erythroleukemia cells, plated them in soft agar containing G418, selected for 2 to 3 weeks, and counted colonies (Fig. 1). When placed between the enhancer and promoter, the *Rasgrf1* DMD and repeats together reduced the colony number regardless of their orientation. The magnitude of this reduction was comparable to that provided by the enhancer blocker found at the chicken β-globin locus (3). In contrast, the *Rasgrf1* sequences did not reduce the colony number when placed outside the enhancer-to-promoter interval, indicating that the reduction in colony number was due to enhancer-blocking activity and not nonspecific silencing. The DMD alone exhibited enhancer-blocking activity at a level indistinguishable from that of the DMD repeat combination. The repeats alone had no blocking activity and in fact provided significant but modest stimulation of the colony number in the forward orientation. The numbers of G418-resistant colonies produced by pNI electroporation into K562 cells had been shown to be unaffected by changes in enhancer-to-promoter spacing caused by insertion of sequences from λ phage (3). Collectively, the data indicate the *Rasgrf1* enhancer blocking activity resides in the DMD.

CTCF binding at *Rasgrf1*. Vertebrate enhancer blockers have been shown to require CTCF binding for their activity (3). Furthermore, an enhancer blocker in the *H19* DMD has been shown to bind CTCF in a methylation-sensitive manner, and abrogation of binding by mutation of the binding sites or depletion of CTCF has been shown to eliminate *Igf2* imprinting (2, 10, 13, 21, 25). This led to the model that lack of maternal methylation at the *H19* DMD silences the maternal *Igf2* allele by supporting CTCF binding and enhancer-blocking activity, which prevents the 3′ enhancers from interacting with the 5′ *Igf2* promoters (2). We asked if the *Rasgrf1* DMD also binds CTCF in a methylation-sensitive manner using two independent assays.

First, we performed gel shift experiments using CTCF-containing extracts from chicken erythrocytes, oligonucleotide probes from the DMD, and anti-CTCF antibody to supershift

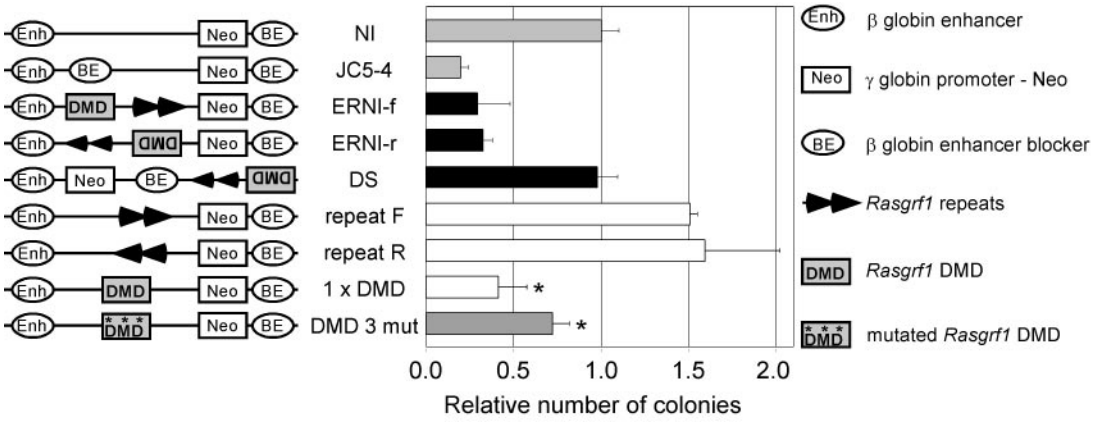

FIG. 1. The *Rasgrf1* DMD has enhancer-blocking activity that depends upon CTCF binding sites. The enhancer-blocking test constructs shown at the left were prepared and transfected into K562 cells as described previously (3, 6). Each contained the chicken β-globin enhancer (Enh), the human ^{A}γ-globin promoter directing transcription of a *neo* reporter (Neo), the chicken β-globin enhancer blocker (BE), and various test fragments. Each test was done 2 to 23 times. The colony number for each test is expressed relative to the number observed with the negative control plasmid (NI) (3), which lacked test sequences and produced an average of 226 colonies. JC5-4 containing the chick β-globin enhancer blocker served as a positive control (7). *Rasgrf1* sequences tested included the DMD and repeats (two black triangles) in both orientations or downstream of the *neo* reporter, one copy of the DMD alone (1 × DMD), and a mutated DMD carrying mutations in the three known CTCF sites (designated 160, 230, and 320 in Fig. 2). Colony counts from 1 × DMD and the DMD with repeats are not significantly different. The difference between results for 1 × DMD and the mutant DMD 3 mut is significant (∗, $P = 0.008$ by t test).

CTCF complexes (Fig. 2A). Three CTCF binding sites were detected within the DMD. One of these (320) bound CTCF, more effectively than the other two. We used the 320 oligonucleotide in additional gel shift experiments using purified chicken CTCF and competitor probes (Fig. 2B). Competitors included self, a methylated form of self, CTCF sites from the mouse *H19* and chicken β-globin loci, as well as mutated forms of the chicken β-globin probes. CTCF binding to the *Rasgrf1* DMD 320 site was completely blocked by the *H19* and wild-type chicken β-globin competitors and partially blocked by self and a mutated form of the chicken β-globin probe that has attenuated CTCF binding. However, binding was not competed at all by a methylated form of the 320 probe, suggesting CTCF binding to 320 was methylation sensitive. CTCF binding at *H19* and chicken β-globin may be stronger than its binding to *Rasgrf1*.

To confirm that CTCF binds the DMD in a methylation-sensitive manner, gel shift studies were repeated using PCR-generated probes containing the three individual CTCF sites in the DMD that were either methylated or unmethylated (Fig. 2C). Interacting proteins were prepared by in vitro translation of templates encoding CTCF, the Zn-finger domain of CTCF, or luciferase as a negative control. The in vitro-translated CTCF did not bind as well as the native CTCF used in Fig. 2A and B; however, the unmethylated form of each probe bound the CTCF Zn-finger domain. When the probes were methylated, their binding to the CTCF Zn-finger domain was greatly reduced or eliminated altogether, confirming that CTCF binding to the DMD is methylation sensitive (Fig. 2C).

To determine if the CTCF binding sites in the *Rasgrf1* DMD were important for the enhancer-blocking activity, we mutated the three CTCF sites within the DMD we identified, changing each of six conserved nucleotides in those sites with a transition mutation. When we performed gel shift and competition experiments similar to those described above, results showed the mutations diminished, but did not completely abolish, CTCF Zn-finger domain binding (Fig. 2D and E). In enhancer-blocking assays, the DMD that was mutated at all three CTCF sites was significantly less effective at blocking the enhancer-to-promoter interactions than the wild-type DMD (Fig. 1), though enhancer blocking activity was not eliminated. This may be due to residual CTCF binding activity in the mutated sites or additional CTCF sites within the DMD that we did not find.

We extended these results to confirm that the *Rasgrf1* DMD binds CTCF in a methylation-sensitive manner and that binding occurs at the *Rasgrf1* locus in cells and not only to synthetic probes in biochemical tests. For these assays, we performed ChIP experiments (Fig. 2F) using embryonic fibroblasts from heterozygous mice with a maternally (−/+) or paternally (+/−) derived repeat deletion (29). All precipitated material was analyzed by a PCR assay specific for the wild-type allele. This enabled us to separately monitor CTCF binding to the wild-type paternal allele, which is methylated in −/+ cells, and the wild-type maternal allele, which is unmethylated in +/− cells (Fig. 2G). This assay does not detect the mutated (−) allele. Consistent with our gel shift data, we could not detect CTCF binding to the methylated, wild-type, paternal DMD in −/+ cells. However, when we looked for binding to the unmethylated, wild-type maternal DMD in +/− cells, CTCF binding was readily detected. This too was consistent with our gel shift data showing that CTCF binds to its sites in the *Rasgrf1* DMD when they are unmethylated.

Collectively, these studies indicate that the *Rasgrf1* DMD is a methylation-sensitive enhancer blocker that silences the unmethylated maternal allele by binding CTCF. The methylated paternal allele is expressed because repeat-induced methylation prevents CTCF binding at *Rasgrf1*.

Enhancer location controls *Rasgrf1* imprinting. We wondered if imprinted expression of *Rasgrf1* in vivo in fact relies

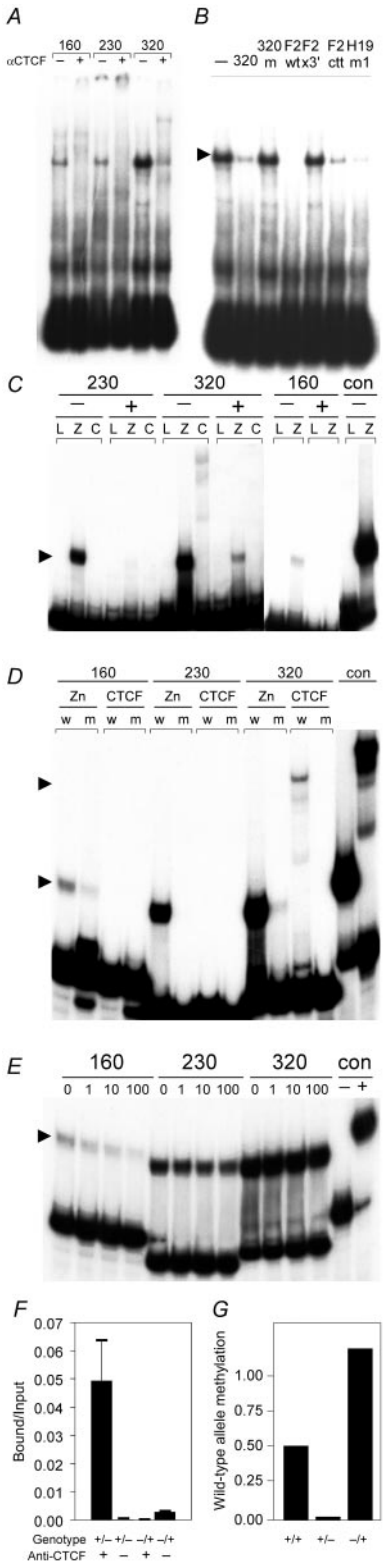

FIG. 2. CTCF binds the unmethylated *Rasgrf1* DMD. A. Oligonucleotide probes corresponding to three sequences in the DMD (230, 320, and 160) were tested for CTCF binding by gel shift analysis. Reactions included CTCF-containing extracts from chicken erythrocytes with (+) or without (−) anti-CTCF antibody. B. One of the probes (320) was used in further gel shift experiments using CTCF purified from chicken erythrocytes and several competitor probes. Binding reactions were done with no competing oligonucleotide (−) or 200-fold molar excesses of competitors that included self (320), methylated self (320m), the wild-type CTCF binding site at the chicken β-globin locus (F2wt), mutated forms of the chicken β-globin CTCF site that abolished (F2x3′) or attenuated (F2ctt) CTCF binding, and a CTCF site from *H19*. C. Methylation-sensitive binding was confirmed using larger probes containing the three *Rasgrf1* CTCF sites prepared by PCR and methylated in vitro (+) or left unmethylated (−) prior to incubation with in vitro-transcribed and -translated luciferase (L), Zn-finger domain of CTCF (Z), or full-length CTCF (C). An unmethylated human *XIST* probe (con) was used as a positive control for binding. D. Probes generated by PCR corresponding to wild-type (w) or mutated (m) forms of *Rasgrf1* CTCF sites 160, 230, and 320 were tested for binding to the in vitro-translated and -transcribed Zn-finger domain of CTCF. The mutated forms of these sites were those used in enhancer-blocking tests in Fig. 1. E. The wild-type probes from panel D were used in competition assays that included the Zn-finger domain of CTCF and increasing molar excesses (0 or 1-, 10-, or 100-fold) of unlabeled, mutated site probes. An unmethylated human *XIST* probe (con) was used with (+) or without (−) added protein as a control. Arrowheads in panels B, C, D, and E indicate positions of complexes with the full-length CTCF or Zn-finger domain complexes. F. Chromatin immunoprecipitation was performed using embryonic fibroblasts from mice with a paternally (+/−) or maternally (−/+) inherited repeat deletion (29) with (+) or without (−) antibody against CTCF. Precipitates were analyzed using real-time PCR with primers specific for the wild-type allele only. The experiment was done in triplicate, and the fraction of input that was precipitated is reported. Error bars show the standard deviation. G. The methylation state of HhaI sites in the wild-type allele was measured by real time PCR. DNAs from wild-type (+/+), +/−, and −/+ cells used in panel F were amplified with wild-type-specific primers that spanned five HhaI sites in the DMD. Amplification was done either before or after digestion with HhaI. Wild-type allele methylation is the ratio of product amplified from the digested templates to that from undigested templates. Of the two wild-type alleles in +/+ cells, only the paternal is methylated (ratio = 0.50), the single wild-type maternal allele in +/− cells is not appreciably methylated (ratio = 0.014), and the single wild-type paternal allele in −/+ cells is fully methylated (ratio = 1.2).

upon regulation of enhancer-to-promoter interactions by the enhancer blocker within the DMD. If this is the case, we reasoned that we should be able to bypass the imprinting switch altogether by placing an extra enhancer downstream of the DMD repeat interval. At this location, the enhancer could interact with the promoter, unencumbered by an intervening enhancer blocker, enabling the modified allele to escape imprinting control. We tested this hypothesis using two independently derived mouse mutants. In one mutant, we deleted the *Rasgrf1* repeats and replaced them with a *neo* cassette containing a 500-bp transcriptional control sequence from the mouse *Pgk* gene (Fig. 3A and B). The 500-bp sequence contains the *Pgk* promoter as well as the enhancer (19). We designated this extra enhancer allele *Rasgrf1*^{tm2Pds}. Consistent with our earlier studies (29), removal of the paternal repeats caused a loss of paternal allele methylation. This was shown by Southern blot analysis of the NotI site in the DMD (Fig. 3C) and by bisulfite analysis of 19 CpGs in the paternal DMD (data not shown). These results using an allele independent of the one described in our earlier studies (29) verified that the repeats positively regulate paternal allele DNA methylation at *Rasgrf1*.

When we monitored *Rasgrf1* expression in mice carrying the extra enhancer by using an allele-specific assay, we observed that the enhancer insertion enabled expression of *Rasgrf1* re-

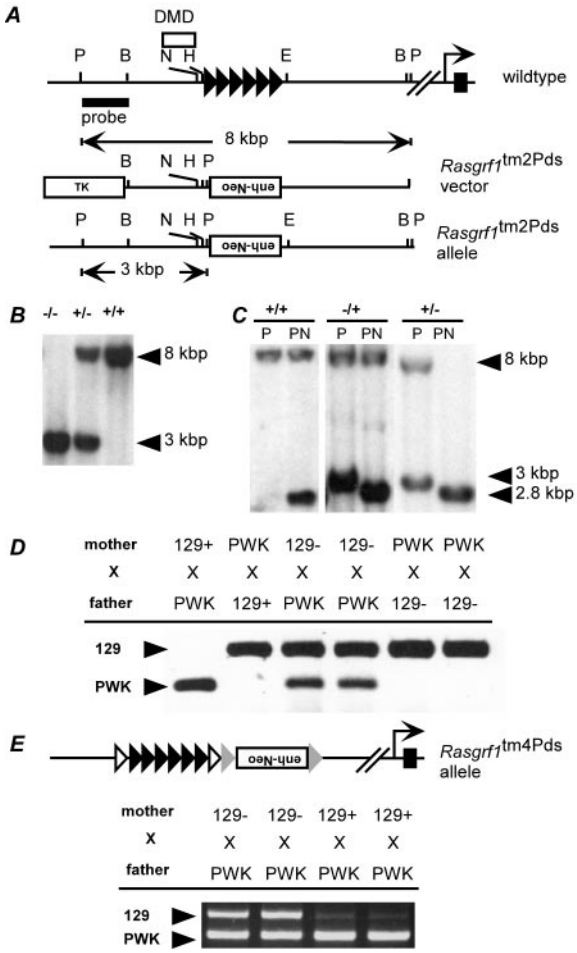

FIG. 3. An extra enhancer at *Rasgrf1* bypasses imprinted regulation caused by the DMD enhancer-blocking element. A. The wild-type *Rasgrf1* locus was mutated to create a new allele (*Rasgrf1*^{tm2Pds}) that placed an enhancer (enh-neo) in an inverted orientation at the locus in place of the repeats (filled triangles). B. Southern blot analysis using the probe shown in panel A and PstI-digested DNA revealed the expected 8.0-kbp and 3.0-kbp bands from the wild-type (+) and mutated (−) alleles, respectively, confirming homologous recombination. C. Methylation analysis by Southern blotting using PstI (P) and NotI (N) produced a 2.8-kbp band when methylation was absent from either the wild-type or mutated allele. Maternal transmission of the *Rasgrf1*^{tm2Pds} allele (−/+) had no effect on methylation, while in mice with paternal transmission (+/−), the sole band at 2.8 kbp indicated that methylation of the paternal allele was lost. D. Allele-specific reverse transcriptase PCR using cDNA prepared from neonatal brains of progeny from reciprocal crosses between wild-type PWK mice and animals with the *Rasgrf1*^{tm2Pds} mutation on the 129S4/SvJae (129) background. The extra enhancer-containing *neo* cassette facilitated expression of the otherwise silent maternal allele when it was maternally transmitted and enabled paternal allele expression even though paternal methylation was absent. E. Expression analysis of an independently derived allele with *loxP* sites (open triangles) flanking the repeats and *frt* sites (shaded triangles) flanking the *enh-neo* cassette (*Rasgrf1*^{tm4Pds}) (R. Holmes et al., submitted) revealed the same escape from imprinted expression as for the *Rasgrf1*^{tm2Pds} allele.

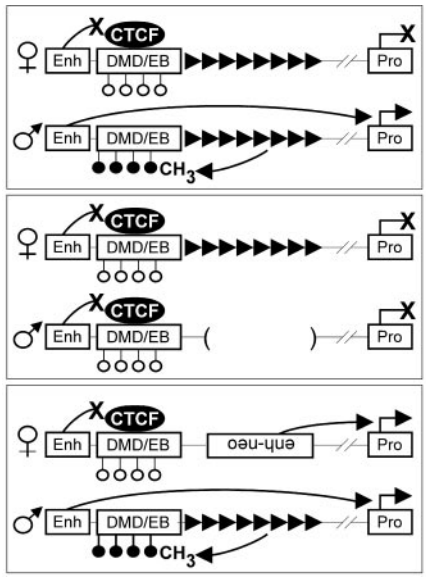

FIG. 4. Model depicting the *Rasgrf1* DMD and repeat as a binary switch that regulates *Rasgrf1* imprinting. Shown are the putative neonatal enhancer (Enh), promoter (Pro), repeats (rightward-pointing filled triangles) and the DMD methylated (filled circles) and unmethylated (open circles) on the paternal and maternal alleles, respectively. Curved lines ending in an X indicate blocked interactions or activities, and lines ending in an arrowhead indicate those that are permitted. The repeat-deficient *Rasgrf1* allele (*Rasgrf1*^{tm1Pds}) was described earlier (29). See the text for details.

gardless of whether it was transmitted maternally or paternally (Fig. 3D). Expression was due entirely to the presence of the *Pgk-enh-pro-neo* insertion and not due to repeat deletion, because mice with only a repeat deletion and no enhancer-containing *Pgk-neo* cassette failed to express *Rasgrf1* from the mutated allele (29). Importantly, while DMD methylation is normally required for expression of *Rasgrf1* in neonatal brain, the extra enhancer allowed expression even in the absence of methylation.

The results from the *Rasgrf1*^{tm2Pds} mutation were confirmed by analysis of another independent mutation we prepared in which the enhancer-containing cassette was inserted 3′ of the *Rasgrf1* repeats (Fig. 3E) (Holmes et al., submitted). In these mice, the maternal allele was also activated by the cassette insertion, demonstrating that the *Pgk-enh-pro-neo* insertion bypassed imprinted expression of *Rasgrf1* whether the repeats were present or not. These results, in combination with the in vitro results described above, indicated the enhancer-blocking activity of the *Rasgrf1* DMD is central to regulation of *Rasgrf1* imprinting in vivo. Enhancer relocation studies at *H19* similarly supported the model that *Igf2* is regulated by the methylation-sensitive enhancer blocker in the *H19* DMD (28).

Model for *Rasgrf1* imprinting. In the female germ line of wild-type mice (Fig. 4, top), the *Rasgrf1* repeat element does not induce DMD methylation and the unmethylated allele transmitted from mother to progeny binds CTCF. CTCF binding facilitates the enhancer-blocking activity of the DMD, which prevents a yet-to-be-identified upstream enhancer from stimulating *Rasgrf1* transcription in neonatal brain, and the maternal allele is silent. In the male germ line, the *Rasgrf1* repeat element establishes methylation at the DMD. The methylated allele transmitted from father to progeny maintains its methylation and cannot bind CTCF. Because CTCF is not bound, the enhancer blocker does not function on the paternal

allele and enhancer-to-promoter interactions are permitted, causing expression of the paternal allele in neonatal brain. In mice carrying the repeat-deficient *Rasgrf1*^{tm1Pds} allele on the paternal chromosome (Fig. 4, middle), normal DMD methylation never becomes established. In this case, neither allele is methylated at the DMD, and CTCF binds both alleles and enables the maternal and paternal enhancer blockers to silence both alleles.

In mice carrying the extra enhancer allele (*Rasgrf1*^{tm2Pds}) on the maternal chromosome (Fig. 4, bottom), the enhancer-blocking function is still active because the DMD is unmethylated and CTCF can bind. But the location of the extra enhancer allows it to bypass regulation by the DMD enhancer blocker and activate the maternal promoter, resulting in biallelic expression. When the mutation is inherited paternally, the DMD fails to become methylated because the repeats are missing (Fig. 3C). The absence of paternal methylation can support CTCF binding and enhancer-blocking activity, which would silence the paternal allele. However, the placement of the extra enhancer bypasses the DMD enhancer blocker, allowing apparently normal expression of the paternal allele (Fig. 3D). This model of imprinted expression is similar to the model described for *H19*/*Igf2* in that allele-specific expression is mediated by a methylation-sensitive enhancer blocker.

DISCUSSION

It is not clear how the *Rasgrf1* repeats regulate paternal DMD methylation. In plants, transcripts that include inverted repeats can be processed into 21- to 25-nt small interfering RNAs (siRNAs) that regulate local DNA methylation (1, 20). Such mechanisms have been reported in mammalian cells, too (16). Furthermore, if models depicting direct repeats as a source for siRNAs are valid (18), then the *Rasgrf1* repeats may regulate local DNA methylation by RNA-mediated mechanisms. However, we have been unable to detect RNAs emanating from the *Rasgrf1* repeats in the siRNA size range (R. Holmes and P. D. Soloway, unpublished data). Second, it is not clear how paternal allele methylation is erased in the female germ line. This may be a passive process in which methylation is not maintained during female germ line development, but it may be an active process, involving local *cis*-acting methyl erasure signals. Transgenic studies suggest that the *Rasgrf1* repeats are sufficient for paternal allele methylation of the DMD, but additional sequences are necessary for demethylation of the maternal *Rasgrf1* allele (H. Herman, B. Hu, and P. D. Soloway, unpublished data). There is precedent for the existence of such demethylating signals at *Snrpn* (26).

It is clear that mechanisms governing imprinted methylation are varied and that no one unifying mechanism applies to all loci. This is true even if one considers only imprinted methylation at paternal alleles. For example, key differences exist between paternal methylation of *Rasgrf1* and *H19*. Notably, regulation of methylation at *Rasgrf1* is by a positive mechanism requiring the repeats. Without the repeats, no methylation is established. At *H19*, no positive regulators for establishing DMD methylation have been identified. In fact, it is possible that methylation is the default state at the paternal *H19* DMD and that methylation is inhibited at the maternal allele by a CTCF-dependent mechanism (8, 21, 22, 25). Studies of *Dnmt3a* mutant mice also reveal multiple mechanisms for establishing paternal allele methylation. In primordial germ cells taken from male mice lacking DNMT3a, it was shown that *H19* and the intergenic DMD at *Dlk1-Gtl2* failed to acquire methylation normally seen there, yet *Rasgrf1* became methylated (14). Although this suggests a common DNMT requirement for *H19* and *Dlk1-Gtl2* and a different one for *Rasgrf1*, *H19* methylation also required *Dnmt3L*, but *Dlk1-Gtl2* did not. These results illustrate that paternal methylation at each of these imprinted loci involves distinct mechanisms.

Three details regarding imprinted expression of *Rasgrf1* are missing. First, it is not clear if the DMD contains additional CTCF binding sites other than the three we identified. The DMD with mutations in the three CTCF sites still had blocking activity, although it was significantly less than the blocking activity of the wild-type DMD. The residual blocking activity could be due to additional CTCF binding sites we did not find or because the mutations at positions 160 and 230 did not completely abolish CTCF binding (Fig. 2D and E). Second, the evidence for enhancers controlling *Rasgrf1* expression remains circumstantial: we have yet to identify the endogenous enhancer(s) for *Rasgrf1* expression that are regulated by the enhancer-blocking activity of the DMD. Because locating an extra enhancer 3′ of the DMD ablates imprinted expression, we looked 5′ of the DMD for enhancers. Sequence comparisons between mouse and human revealed several conserved sequences in this region. Similar comparisons at *H19* were used to identify enhancers there (12); however, we were unable to demonstrate enhancer activity for the conserved *Rasgrf1* sequences (R. Holmes, unpublished). Finally, paternal allele-specific expression of *Rasgrf1* is restricted to the neonatal mouse brain. In other tissues and in adult brain, *Rasgrf1* expression is biallelic. Based on our model, we predict that this can happen when the *Rasgrf1* promoter escapes its requirement for an enhancer or when alternate enhancers 3′ of the repeats become active that can bypass the DMD enhancer blocker mechanism because of their location.

The model we present accounts for all imprinting phenotypes described for wild-type mice (23) and for mice with mutations in *Rasgrf1* imprinting control sequences (11, 29) and with all biochemical and cell biological analyses of *Rasgrf1* imprinting described here. This model may guide additional studies to elaborate mechanisms of genomic imprinting at *Rasgrf1*.

ACKNOWLEDGMENTS

We are grateful to Gary Felsenfeld and Shirley Tilghman for helpful discussions.

Funding to P.D.S. was from the National Institutes of Health (CA98596 and EY11279), the U.S. Army (DAMD17-02-1-0652), and the Roswell Park Cancer Institute Alliance. Support was also provided by the National Cancer Institute Cancer Center Support Grant to Roswell Park Cancer Institute (P30CA016056).

REFERENCES

1. **Aufsatz, W., M. F. Mette, J. van der Winden, A. J. Matzke, and M. Matzke.** 2002. RNA-directed DNA methylation in Arabidopsis. Proc. Natl. Acad. Sci. USA **99:**16499–16506.
2. **Bell, A. C., and G. Felsenfeld.** 2000. Methylation of a CTCF-dependent boundary controls imprinted expression of the Igf2 gene. Nature **405:**482–485.
3. **Bell, A. C., A. G. West, and G. Felsenfeld.** 1999. The protein CTCF is required for the enhancer blocking activity of vertebrate insulators. Cell **98:**387–396.

4. **Birger, Y., R. Shemer, J. Perk, and A. Razin.** 1999. The imprinting box of the mouse Igf2r gene. Nature **397:**84–88.
5. **Chaillet, J. R.** 1994. Genomic imprinting: lessons from mouse transgenes. Mutat. Res. **307:**441–449.
6. **Chung, J. H., A. C. Bell, and G. Felsenfeld.** 1997. Characterization of the chicken beta-globin insulator. Proc. Natl. Acad. Sci. USA **94:**575–580.
7. **Chung, J. H., M. Whiteley, and G. Felsenfeld.** 1993. A 5′ element of the chicken beta-globin domain serves as an insulator in human erythroid cells and protects against position effect in Drosophila. Cell **74:**505–514.
8. **Fedoriw, A. M., P. Stein, P. Svoboda, R. M. Schultz, and M. S. Bartolomei.** 2004. Transgenic RNAi reveals essential function for CTCF in H19 gene imprinting. Science **303:**238–240.
9. **Filippova, G. N., S. Fagerlie, E. M. Klenova, C. Myers, Y. Dehner, G. Goodwin, P. E. Neiman, S. J. Collins, and V. V. Lobanenkov.** 1996. An exceptionally conserved transcriptional repressor, CTCF, employs different combinations of zinc fingers to bind diverged promoter sequences of avian and mammalian c-*myc* oncogenes. Mol. Cell. Biol. **16:**2802–2813.
10. **Hark, A. T., C. J. Schoenherr, D. J. Katz, R. S. Ingram, J. M. Levorse, and S. M. Tilghman.** 2000. CTCF mediates methylation-sensitive enhancer-blocking activity at the H19/Igf2 locus. Nature **405:**486–489.
11. **Herman, H., M. Lu, M. Anggraini, A. Sikora, Y. Chang, B. J. Yoon, and P. D. Soloway.** 2003. Trans allele methylation and paramutation-like effects in mice. Nat. Genet. **34:**199–202.
12. **Ishihara, K., N. Hatano, H. Furuumi, R. Kato, T. Iwaki, K. Miura, Y. Jinno, and H. Sasaki.** 2000. Comparative genomic sequencing identifies novel tissue-specific enhancers and sequence elements for methylation-sensitive factors implicated in Igf2/H19 imprinting. Genome Res. **10:**664–671.
13. **Kanduri, C., V. Pant, D. Loukinov, E. Pugacheva, C. F. Qi, A. Wolffe, R. Ohlsson, and V. V. Lobanenkov.** 2000. Functional association of CTCF with the insulator upstream of the H19 gene is parent of origin-specific and methylation-sensitive. Curr. Biol. **10:**853–856.
14. **Kaneda, M., M. Okano, K. Hata, T. Sado, N. Tsujimoto, E. Li, and H. Sasaki.** 2004. Essential role for de novo DNA methyltransferase Dnmt3a in paternal and maternal imprinting. Nature **429:**900–903.
15. **Kantor, B., K. Makedonski, Y. Green-Finberg, R. Shemer, and A. Razin.** 2004. Control elements within the PWS/AS imprinting box and their function in the imprinting process. Hum. Mol. Genet. **13:**751–762.
16. **Kawasaki, H., and K. Taira.** 2004. Induction of DNA methylation and gene silencing by short interfering RNAs in human cells. Nature **431:**211–217.
17. **Li, E., C. Beard, and R. Jaenisch.** 1993. Role for DNA methylation in genomic imprinting. Nature **366:**362–365.
18. **Martienssen, R. A.** 2003. Maintenance of heterochromatin by RNA interference of tandem repeats. Nat. Genet. **35:**213–214.
19. **McBurney, M. W., L. C. Sutherland, C. N. Adra, B. Leclair, M. A. Rudnicki, and K. Jardine.** 1991. The mouse Pgk-1 gene promoter contains an upstream activator sequence. Nucleic Acids Res. **19:**5755–5761.
20. **Mette, M. F., W. Aufsatz, J. van Der Winden, M. A. Matzke, and A. J. Matzke.** 2000. Transcriptional silencing and promoter methylation triggered by double-stranded RNA. EMBO J. **19:**5194–5201.
21. **Pant, V., S. Kurukuti, E. Pugacheva, S. Shamsuddin, P. Mariano, R. Renkawitz, E. Klenova, V. Lobanenkov, and R. Ohlsson.** 2004. Mutation of a single CTCF target site within the H19 imprinting control region leads to loss of Igf2 imprinting and complex patterns of de novo methylation upon maternal inheritance. Mol. Cell. Biol. **24:**3497–3504.
22. **Pant, V., P. Mariano, C. Kanduri, A. Mattsson, V. Lobanenkov, R. Heuchel, and R. Ohlsson.** 2003. The nucleotides responsible for the direct physical contact between the chromatin insulator protein CTCF and the H19 imprinting control region manifest parent of origin-specific long-distance insulation and methylation-free domains. Genes Dev. **17:**586–590.
23. **Plass, C., H. Shibata, I. Kalcheva, L. Mullins, N. Kotelevtseva, J. Mullins, R. Kato, H. Sasaki, S. Hirotsune, Y. Okazaki, W. A. Held, Y. Hayashizaki, and V. M. Chapman.** 1996. Identification of Grf1 on mouse chromosome 9 as an imprinted gene by RLGS-M. Nat. Genet. **14:**106–109.
24. **Pugacheva, E. M., V. K. Tiwari, Z. Abdullaev, A. A. Vostrov, P. T. Flanagan, W. W. Quitschke, D. I. Loukinov, R. Ohlsson, and V. V. Lobanenkov.** 2005. Familial cases of point mutations in the XIST promoter reveal a correlation between CTCF binding and pre-emptive choices of X chromosome inactivation. Hum. Mol. Genet. **14:**953–965.
25. **Schoenherr, C. J., J. M. Levorse, and S. M. Tilghman.** 2003. CTCF maintains differential methylation at the Igf2/H19 locus. Nat. Genet. **33:**66–69.
26. **Shemer, R., A. Y. Hershko, J. Perk, R. Mostoslavsky, B. Tsuberi, H. Cedar, K. Buiting, and A. Razin.** 2000. The imprinting box of the Prader-Willi/Angelman syndrome domain. Nat. Genet. **26:**440–443.
27. **Thorvaldsen, J. L., K. L. Duran, and M. S. Bartolomei.** 1998. Deletion of the H19 differentially methylated domain results in loss of imprinted expression of H19 and Igf2. Genes Dev. **12:**3693–3702.
28. **Webber, A. L., R. S. Ingram, J. M. Levorse, and S. M. Tilghman.** 1998. Location of enhancers is essential for the imprinting of H19 and Igf2 genes. Nature **391:**711–715.
29. **Yoon, B. J., H. Herman, A. Sikora, L. T. Smith, C. Plass, and P. D. Soloway.** 2002. Regulation of DNA methylation of Rasgrf1. Nat. Genet. **30:**92–96.